Simulating 3-D water flow in subsurface drain trenches and surrounding soils in a clayey field

Heidi Salo[a], Lassi Warsta[b], Mika Turunen[b], Jyrki Nurminen[c], Merja Myllys[d], Maija Paasonen-Kivekäs[e], Laura Alakukku[f], Harri Koivusalo[b]

[a] Corresponding author information: tel. +358 505307604, email: heidi.salo@aalto.fi, Aalto University School of Engineering, Department of Built Environment, P.O. Box 15300, FI-00076 Aalto, Finland.

[b] Aalto University School of Engineering, Department of Built Environment, P.O. Box 15300, FI-00076 Aalto, Finland.

[c] The Finnish Field Drainage Association, Simonkatu 12 A 11, FI-00100 Helsinki, Finland.

[d] Natural Resources Institute Finland, Tietotie 4, FI-31600 Jokioinen, Finland.

[e] Sven Hallin Research Foundation, Simonkatu 12 A 11, FI-00100 Helsinki, Finland.

[f] University of Helsinki, Dep. of Agricultural Sciences, P.O. Box 28, FI-00014 University of Helsinki.

Abstract

Subsurface drain trenches are important pathways for water movement from the field surface to subsurface drains in low permeability clayey soils. The hydrological effects of trenches installed with well conducting backfill material and gravel inlet patches are difficult to study with only experimental methods. Computational three-dimensional soil water models provide additional tools to assess spatial processes of such drainage system. The objective was to simulate water flow pathways with 3-D FLUSH model in drain spacing and trench depth scale with two model configurations: (1) the total pore space of soil was treated as a single continuous pore system and (2) the total pore space was divided into mobile soil matrix and macropore systems. Both model configurations were parametrised almost solely with field data without calibration. Data on soil hydraulic properties and drain discharge measurements were available from a clayey subsurface drained agricultural field in southern Finland. The effect of soil hydraulic variability on water flow pathways was assessed by generating computational grids in which the hydraulic properties were sampled randomly from five measured soil sets. Both model configurations were suitable to describe the recorded drain discharge, when model was parameterized in finer scale than drain spacing and the parameterization described highly conductive subdomains such as macropores in dual-permeability model or the trench in single pore system model. Models produced similar hourly discharge and water balance results with randomly sampled soil hydraulic properties. The results provide a new view on consequences of soil heterogeneity on subsurface drainage. The practical implication of the results from different drainage scenarios is that gravel trench appears to be important only in soils with a poorly conductive subsoil layers without direct macropore connections to subsurface drains. Solely drain discharge data was not sufficient to determine the differences in water flow pathways between the two model configurations and more output variables, such as groundwater level, should be taken into account in making assessments on the effects of different drainage practices on field drainage capacity.

Keywords

3-D modeling; preferential flow; supplementary drain installation

1. Introduction

Cultivated clayey soils are abundant in the coastal areas of the Baltic Sea and they are routinely subsurface drained to remove excess water from the fields during wet autumn and spring snow melt periods. Efficient drainage reduces the risk of soil compaction due to machine traffic during field operations after moist periods (e.g. Alakukku et al., 2003) and prevents waterlogging in the root zone during the growing season. In Nordic countries, subsurface drains are installed mainly with the trenchless or trench installation methods (e.g. Ritzema et al., 2006). In the trench installation method, a trench is excavated with a machine, and simultaneously the drain pipe is laid at the bottom of the trench. The pipe is covered using an envelope material such as gravel and the trench is filled with a mixture of tilled topsoil and subsoil (e.g. Stuyt et al., 2005).

In low permeability soils, such as clays, the main function of envelope material is to improve permeability around the pipe (Stuyt et al., 2005) and the drain trenches provide a well conducting pathway for water from the field surface to the subsurface drains. Gravel inlets, created by pouring gravel into the trench up to the topsoil layer, are often used to increase the conductivity of the backfill material even though their effect is somewhat controversial (Aura, 1990). The functioning of the trench and drain envelope material appears to depend on the characteristics of the surrounding soil (Ritzema et al., 2006; Stuyt et al., 2005) but this has only rarely been studied in detail. Turtola and Paajanen (1995) noticed that drain installation with wooden chips and topsoil in the drain trenches increased drain discharge compared to the situations with impermeable subsoil and gravel envelope around the drain pipe. Messing and Wesström (2006) found that differences in soil properties between the trench material and the surrounding soil layers control the formation of drain discharge in old drainage systems, as fast flow through the drain trench was combined with a more gradual release of water from the surrounding soil layers.

The clay soil matrix usually conducts water poorly but cracks, pores between aggregates, and macropores composed of plant root channels and earthworm burrows provide additional flow capacity for percolating water. The tilled topsoil layer is well conductive due to the impact of tillage operations on soil hydraulic conductivity and macroporosity (e.g. Turtola et al., 2007). Field drainage affects the soil structure development in heavy clay soils and enhances the formation of soil aggregates and preferential flow pathways (e.g. Alakukku et al., 2010). Preferential flow pathways allow rapid movement of water (Jarvis, 2007) and generate the main part of drain discharge in clayey soils (e.g. Frey et al., 2016; Warsta et al., 2013). When gravel envelope material is used in macroporous soil, the role of preferential flow and the envelope for field drainage is unclear.

Macroporosity of soils appears to vary spatially and it has been shown with soil sample analyses and tracer experiments that more earthworm burrows and root channels exist above the drains, partly due to more suitable moisture conditions than elsewhere in the field (Alakukku et al., 2010; Shipitalo et al., 2004; Nuutinen et al., 2003). Direct connections between the drains and the soil surface have been verified by injecting smoke into drainpipe outlets and mapping the locations where the smoke billowed out of the soil (Nielsen et al., 2015). Messing and Wesström (2006) reported that in fields with 2 to 45 years old drain systems hydraulic conductivities were higher in the trench backfill soil compared to the soil between the drains. Alakukku et al. (2010) studied a heavy clay field with 50-year-old drainage system and demonstrated spatial variability in soil macroporosity and hydraulic conductivity, but found no notable differences in these variables between locations above the drain line and in the midpoint of the drain lines. The literature reports about spatial differences in preferential flow paths and provides some conceptual understanding of their implications on subsurface flow, but quantitative assessment of their role calls for application of simulation models. Messing and Wesström (2006) suggest that simulations of water flow in these heterogeneous soils should take into account the quick water flow to drainpipes in the permeable backfill material and slower, more continuous water flow from the soil layers between the trenches.

Hydrological models are regularly used to analyze the performance of field drainage systems (e.g. Nousiainen et al., 2015; Turunen et al., 2013). Two-dimensional (2-D) and three-dimensional (3-D) models can take into account the topography and spatial variability of soil hydraulic characteristics (e.g. Haws et al., 2005; Hansen et al., 2013; Klaus and Zehe, 2010; Henine et al., 2014; De Schepper et al., 2015; Turunen et al., 2015a) and thus simulate the hydrological effect of a trench (Gärdenäs et al., 2006) and features such as mole drains or gravel inlets that lie in the trench at regular intervals (Filipović et al., 2014).

Several 1-D (Jarvis and Larsbo, 2012; Jansson and Karlberg, 2004; van Dam, 2008), 2-D (Abrahamsen and Hansen, 2000) and 3-D (Danish Hydraulic Institute (DHI), 2007; Šimůnek and van Genuchten, 2008; Warsta et al., 2013; Brunner and Simmons, 2012) models which include descriptions of preferential flow processes have been developed. A common approach to simulate preferential flow is to divide the soil porosity into two or more pore systems, e.g. soil matrix and macropores that conduct water at different rates and can exchange water between the systems (e.g. Köhne and Mohanty, 2006). Another approach to take preferential flow into account in computational models is to apply single pore system models with explicit representation of the macropores as high flow numerical units (e.g. Klaus and Zehe, 2010; Vogel et al., 2000). Parameterization of preferential flow models can be challenging because the related parameter values can be difficult to derive from laboratory data (e.g. Gärdenäs et al., 2006; Haws et al., 2005; Köhne and Mohanty, 2006). Previous studies have successfully simulated water flow in clay soils, but challenges remain with model parameterization and description of preferential flow processes (Beven and German, 2013).

Models that include a preferential flow description can give insight whether the effect of macropores on water flow is crucial in the simulated soil domain (Gärdenäs et al., 2006; Klaus and Zehe, 2010). According to Vogel et al. (2000), the effect of soil heterogeneity could be described with a dual-permeability model or with a single pore system model where soil hydraulic parameters are randomized. There is a need to compare the suitability of different pore system approaches.

In this study we strived to clarify the role of drain trenches, gravel envelope material and soil macropores in the formation of drain discharge in clay soil with different hydraulic properties. We simulated 3-D water flow in drain spacing scale with the FLUSH model that supported direct parameterization of drain trenches in heterogeneous clayey soils. Our objective was to investigate if the model can reproduce the drain discharge with 1) a single pore system and 2) dual-permeability configurations when the values of the hydraulic parameters are taken from measurements and are not calibrated. The study setup enabled us to investigate if the application of the two model configurations using the same data set can give insight on water flow pathways in drain spacing scale. Our hypothesis is that in clayey soils water initially flows laterally in the tilled topsoil layer towards the trench and to the drainpipe. Presumably the effect of the drain trench increases as the saturated hydraulic conductivity of the surrounding soil decreases.

2. Materials and methods

2.1. Site and data description

The Nummela experimental site is a subsurface drained clayey field located in Jokioinen (60°51′ 59″N 23°25′ 50″E) southern Finland (Fig. 1a) administrated by the Natural Resources Institute

Finland. The total field area is 9.2 ha and the field is relatively flat (slope < 1%). The experimental field was originally subsurface drained in 1952 with the trench installation method. The drainage system was composed of tile drains (inner diameter 0.05 m), and the drains were installed into a depth of approximately 1.0 m with drain spacings of 16 m (5.8 ha) and 32 m (3.4 ha).

The field area was divided in 2006 into four separately monitored sections (A, B, C and D), where impact of different drainage installation methods on field hydrology, nutrient losses and crop yield were studied before and after the installations (Vakkilainen et al., 2008; 2010; Äijö et al., 2014). The field sections were delineated on the basis of subsurface drainage networks having uniform depth and spacing within each section. Data from section C (1.7 ha) with original drain spacing of 16 m was used in this study.

In June 2008, the trench installation was applied in section C (Äijö et al., 2014) as supplementary drains were installed between the original drains resulting in a drain spacing of 8 m (Fig. 1b). Gravel was used as an envelope material (0.3–0.4 m above the drain) and gravel inlets were installed into the trench with a spacing of 7–8 m. The monitoring of the field section was started one year before the drainage installation.

Spring barley (*Hordeum vulgare*) and oats (*Avena sativa*) were cultivated in the field section during the study years. Minimum tillage (autumn stubble cultivation with cultivator to 0.10−0.15 m depth) was applied in the section in the autumns except for 2012 due to excessive wetness in the field. The crops were harvested in September except in 2012 when the harvest was postponed into October. The experimental activities and the field setup are reported in more detail in Vakkilainen et al. (2008, 2010) and Äijö et al. (2014).

Soil in section C is classified as Vertic Luvic Stagnosols (IUSS Working Group WBR, 2014) with a mean clay content (particle size < 2 μm) of 66% in the soil layers 0–0.35m and 70–73% in the soil layers 0.35–1m (Vakkilainen et al., 2010). Undisturbed soil cores (diameter 0.15 m and length 0.6

m) were gathered in 2006 with a tractor auger from five locations between the tile drains (Fig. 1b) with 8 m distance to the drains. The cores were divided into three soil samples with an equal height of 0.2 m representing topsoil, plow pan and subsoil layers. Bulk density (Blake and Hartge, 1986), soil porosity and pore size distribution (Danielson and Southerland, 1986; Williams and Shaykewich, 1969), saturated hydraulic conductivity (Youngs, 1991) and water retention characteristics (WRC) (Aura, 1990) were measured on the samples (Table 1). Macropores were defined as pores, which drained in a suction pressure of 0.1 m (diameter >300 μm).

Topsoil layer runoff and drain discharge were measured automatically from section C (Fig. 1b) with a 15 min interval using Datawater WS Vertical helix meter (Maddalena, Povoletto, Italy). Topsoil layer runoff was collected from the downslope side of section C with 0.4 m deep gravel-filled drain trench. Groundwater levels were measured biweekly from nine observation wells (five before supplementary drain installation) installed into a depth of 1.6 m and one into a depth of 2.6 m. Soil (0–0.3 m) water content was measured biweekly at the locations of the groundwater wells with the TRASE system I moisture meter time domain reflectometry sensor (Soil Moisture Equipment Corporation, Coleta, CA, USA). Precipitation was measured on site with a 15 min interval using the RAINEW 111 tipping bucket rain gauge (RainWise Inc., Bar Harbor, ME, USA).

For the calculation of the Penman-Monteith potential evapotranspiration (PET) hourly meteorological data including air temperature, wind speed, incoming solar radiation, and relative humidity were available 5 km from the study site at the Jokioinen Observatory of the Finnish Meteorological Institute (FMI). Missing measurements in the meteorological data set were filled in with values from the Helsinki-Vantaa Airport FMI observatory 100 km from the study site (see Turunen et al., 2015b).

2.2. Model description

FLUSH is an open source 3-D hydrological model developed for simulating water flow (Warsta et al., 2013; Turunen et al., 2013), soil freezing and snow processes (Warsta et al., 2012; Turunen et al., 2015a) in structured soils in Nordic conditions.

The model divides the simulated area into 2-D overland and 3-D subsurface domains. The pore space in the 3-D subsurface domain is either handled as a single continuous pore system or the pore space is divided into two mobile pore systems representing the soil matrix and macropore systems. The dual-permeability approach enables simulation of fast bypass flow of water in the macropore system from the field surface to deeper soil layers.

In the overland domain, water flow on the field surface is described with the diffuse wave approximation of the Saint-Venant equations. Furthermore, the overland domain handles the soil surface depression water storage and sets the upper boundary condition for the subsurface domain. In the model, precipitation is first stored in the soil surface depression storage and overland flow is initiated only after the water depth exceeds the depression storage. Water can be removed from the overland domain by open ditches and infiltration into the subsurface domain. Water can infiltrate into both pore systems of the subsurface domain, but exfiltration back to overland domain is prevented. Water in the subsurface domain can be removed by evapotranspiration, seepage into open ditches, subsurface drains and groundwater outflow.

Water flow in both soil matrix and macropore systems in the subsurface domain are described with the Richards equation. Unsaturated hydraulic conductivity and water retention properties of both pore systems are computed with the van Genuchten (1980) model. The water exchange between the pore systems is driven by pressure differences between the soil matrix and macropores. Water exchange is included as a sink and source term in the Richards equations (Gerke and van Genuchten, 1993):

$$\Gamma = \alpha_W (h_F - h_M) \quad (1)$$

where Γ [T^{-1}] is water exchange rate, α_W [$L^{-1}T^{-1}$] is the first order water exchange coefficient and h [L] is the pressure head in the macropore (F) and matrix (M) systems. The first order water exchange coefficient α_W is defined as follows (Gerke and van Genuchten, 1993):

$$a_W = \frac{\beta}{d^2} K_A \gamma_W \tag{2}$$

where β [-] is a geometry coefficient, d [L] is the distance from soil aggregate to space between the soil aggregates, K_A is the hydraulic conductivity in the matrix-macropore interface and γ_W [-] is a scaling coefficient.

K_A can be computed with various approaches including arithmetic mean of hydraulic conductivities in the soil matrix and macropore systems, minimum or maximum of the conductivities, or using the conductivity of the system, which has the higher pressure head (upwind method) (e.g. An and Noh, 2014).

Computation of drain flux in FLUSH is based on the hydraulic head difference between the surrounding soil and the drainpipe:

$$q_S = K A_S \frac{H_S - H}{\Omega_S} \tag{3a}$$

$$A_S = L_S 2\pi R_S \tag{3b}$$

where q_S [L^3T^{-1}] is the volumetric drain flux, K [L T^{-1}] is the hydraulic conductivity of the matrix or macropore system in the computational cell containing the drainpipe, A_S [L^2] is the drain surface area, H_S is the hydraulic head in the drain, Ω_S [L] is the flow path length, L_S [L] is the drain length in the cell, and R_S [L] is the drain radius. The soil hydraulic conductivity in Eq. 3 is calculated as an arithmetic mean of vertical and horizontal conductivities.

The model calculates evapotranspiration from the subsurface domain based on precomputed PET that is divided into the soil profile according to the root mass distribution. The PET value is decreased in dry conditions with the function of Feddes et al. (1978). Lateral flux of groundwater outflow is removed at the computational domain borders and the hydraulic gradient at the border cell is set equal to the soil surface slope (Warsta et al., 2013).

Implicit finite volume methods are used to discretize the computational domains and numerically solve the governing partial differential equations (PDEs) (Warsta et al., 2013). The overland domain is divided into rectangular cells and the subsurface domain is divided into hexahedric cells with regular curvilinear grids. Unsaturated hydraulic conductivities between computational cells in the subsurface domain are computed with an arithmetic mean of conductivities in two adjacent cells. Backward difference method is used to solve the time derivatives in PDEs.

The simulations are distributed with the MPI (Message Passing Interface) parallelization (Message P Forum, 1994) that divides the simulated domain into subdomains. Each subdomain is laterally surrounded by ghost cells that are need to solve the lateral gradients at the subdomain boundaries during each iteration round. After computing the new hydraulic heads for every cell in each subdomain in one iteration round, the hydraulic head values in the ghost cells are updated with the received values from a neighbor subdomain. Iteration progress information is shared between the subdomains to enable them to stop the process when the hydraulic head changes in the whole domain are below the iteration stop threshold value. The approach enables application of an iterative and continuous solution in the whole simulated domain although each process is only able to access data of the local subdomain.

The original subsurface water flow solver applies the pentadiagonal matrix algorithm to directly solve hydraulic heads in columns of cells in 3-D grids in both pore systems at the same time, and then iteration to solve the horizontal water fluxes between the columns. A new iterative solver was included in the model to solve water flow in the subsurface domain due to numerical stability issues experienced with the original solver. The applied solver uses a Successive Over-Relaxation approach that is a modification of Gauss-Seidel method (Young, 2014).

3. Model setup

The model setup was created to simulate hourly drain discharge before and after supplementary drain installation, and water balances with and without drain trenches in section C of the Nummela field. Three differently parameterized 3-D computational grids (area 8×4 m^2) were prepared for the simulations: (1) a grid with a drain spacing of 16 m including the original trench (Fig. 2a), (2) a grid with a drain spacing of 8 m including the original and supplementary drain trenches (Fig. 2b) and (3) a grid with the drain spacing of 8 m without trenches (Fig. 2c). Since the spacing between the drain lines and gravel inlets was regular and the field is relatively flat, it can be assumed that the hydrological response to the drain installations was similar throughout the section. Thus the length of the simulated domain was set to half of the length of the original drain spacing (8 m) and the width of the domain to half of the distance between the gravel inlets (8 m) (Fig. 2b). Only half of the drainpipe area (Eq. 3) is included in the simulations due to the assumption that the hydrological processes were symmetrical throughout the section. The depth of the grid was 1.5 m reaching below the drain depth of 1.0 m. Grid cell depths in the vertical direction were 0.02 and 0.03 m for the first two layers near the surface and 0.05 m for the layers 3–32. The horizontal cell dimensions were 0.1 m, which was half of the drain trench width (0.2 m). The simulations were conducted with time step lengths of 0.94–3.75 min.

To test the effect of the supplementary drain installation on drain discharge, three rainy autumn periods without crop interaction on field water balance were selected to represent conditions before (1 Oct–4 Nov 2007) and after the installation (14 Oct–7 Nov 2008 and 14 Oct–7 Nov 2012). A two-day model warm-up period was included in the simulated periods. Drain discharge data from the autumn 2007 period was used to test the parameterization of the soil in the original drain trench in grid 1 (Fig. 2a). The drain discharge data from the autumn periods 2008 and 2012 were used to test the capability of the model to reproduce the measured hourly drain discharge results with the measured soil hydraulic properties. Performance of hourly drain discharge simulations was assessed with the Nash-Sutcliffe (N-S) efficiency coefficient (Nash and Sutcliffe, 1970). The simulation results from the autumn 2008 period were further analyzed to decipher differences between the water balances of the grids 1–3 (Figs. 2a–c).

Soil hydraulic parameters (saturated and residual water contents, macroporosity, saturated hydraulic conductivity and van Genuchten water retention curve parameters) required by the model are presented in Table 1. Five soil sets, which included data from the three depths collected from locations C1–C5 (Fig. 1b), were applied one by one to the soil layers outside the drain trench in the simulated periods. The model was run with each soil set and time period for both model configurations.

The bottom soil (1.0–1.5 m) parameterization was derived from previous modelling studies in the Nummela field (Turunen et al., 2013; Salo et al., 2015). We presumed that the original trench backfill material had similar soil parameters as the surrounding clay soil after several decades from the installation in 1952. Hydraulic properties of the original trench soil were computed as an arithmetic average of the topsoil and surrounding soil layer properties (Table 1). Gravel layer of 0.4 m was set on the bottom of the supplementary drain trench (Table 1). At the gravel inlet locations, the depth of the gravel was increased up to the bottom of the topsoil layer. The soil hydraulic parameters of the trench of the new supplemental drains was set according to the measured topsoil

(0–0.2 m) properties, but the gravel layer (0.6–1.0 m) was parameterized after Leij et al. (1996). WRC parameters for the macropore system were set after Köhne and Mohanty (2006).

Randomized soils, where soil properties for the cells between the trenches were assigned by random sampling from Table 1, were created to analyze the hydrological impacts of soil heterogeneity. The randomization was conducted independently for topsoil, plow pan and sub soil layers, e.g. subsoil or plow pan parameterization was not applied for the topsoil layers. The parameterization for the envelope material for the supplementary drain trench and bottom soil material was not randomized.

The same water retention curve was applied in the macropore domain for all the soil layers (Table 1). Measured saturated hydraulic conductivity was decomposed into soil matrix and macropore fractions in the dual-permeability model according to the following equation:

$$K_{sat} = (1.0 - w)K_M + wK_F \qquad (4)$$

$$K_F = K_{FS,MUL}\, w \qquad (5)$$

where K_{sat} [L T^{-1}] is the measured saturated hydraulic conductivity, w [-] is the macroporosity fraction of the total porosity, K_M and K_F [L T^{-1}] are the saturated hydraulic conductivities of the soil matrix and macropore systems, respectively, and $K_{FS,MUL}$ [L T^{-1}] is the macropore saturated hydraulic conductivity multiplier. The value of $K_{FS,MUL}$ in Eq. 5 was initially set to a value of 80 m h^{-1} (Warsta et al., 2013) but was adjusted to assure that the K_M value computed with Eq. 4 was positive. Anisotropy of hydraulic conductivity in macropores was disabled. Parameter values in α_w (Eq. 2) were lumped together into a water exchange coefficient Ψ_w [L^{-2}] except for K_A. The parameter Ψ_w was set to a value of 0.01 m^{-2} in the soil domain (Salo et al., 2015). K_A was computed in the simulations with the upwind method.

Lateral groundwater outflow was triggered at those horizontally outermost grid cells where the terrain slope aspect was directed away from the simulated domain, while groundwater inflow was prevented. The bottom of the grids were considered impermeable. Topsoil layer runoff collector with a length of 8 m was set into depth of 0.4 m and located at the downslope boundary of the domain. Subsurface drains (length 4.0 m) were set into a layer with depth of 0.95–1.0 m (Fig. 2). The pressure values inside the topsoil layer runoff collector and subsurface drainpipe were set to 0.0 m. The value of Ω_S (Eq. 3) was set to 0.1 m, which is the horizontal cell size in the grid. The PET time series was calculated with The Penman–Monteith equation (Allen et al., 1998), similarly as Turunen et al. (2015b).

As initial conditions, overland water depth was set to 0.0 m and groundwater level was derived from observations at five wells in 2007 (average 0.5 m) and nine wells in 2008 (average 0.3 m) and 2012 (average 0.1 m). Initial soil moisture in the unsaturated soil layers was set by assuming static steady state pressure head conditions. The initial conditions were the same for every soil set and both model configurations in each period.

The simulations were run in local workstations and in the Taito supercluster (HP cluster) and Sisu supercomputer (Cray XC30) administered by CSC – IT Center for Science Ltd.

4. Results

The simulation results are presented in three sections: 1) Hourly and 2) cumulative drain discharge results before and after the supplemental drain installation and 3) water balance results for the 2008 period.

4.1. Hourly drain discharge results before and after the supplemental drain installation

Simulations of the 2007, 2008 and 2012 periods were conducted with the two model configurations (single porosity and dual-permeability) and five different soil hydraulic parameterization sets (Table 1). Median of the simulation results with the C1–C5 parameterizations for the single pore and dual-permeability models are presented in Fig. 3 together with the measured series. The two-day model warm-up period is not presented in Fig. 3. Precipitation was 66 mm (33 days), 85 mm (23 days) and 62 mm (23 days) during the 2007, 2008 and 2012 periods, respectively. N-S efficiency coefficients were computed for the median of the simulated results separately for each drain discharge event and model configuration (Fig. 3). The 2007 and 2012 periods were divided into two separate discharge events separated by a dry spell in the middle of the periods. In 2008 autumn precipitation was more evenly distributed resulting in four distinct discharge events.

A clear difference can be seen between the shapes of the measured drain discharge peaks and the simulated peaks (Fig. 3), while both model configurations simulated the timing of the peaks accurately. The highest measured peaks in 2008 and 2012 were blunt and confined to a maximum value of 0.4–0.5 mm h^{-1}, while the simulated peaks with both models were sharper and higher as the single pore model gave a maximum value of 1.0 mm h^{-1} and dual-permeability model 1.6 mm h^{-1}. The peaks produced with the dual-permeability model were almost four times higher than the measured values (Fig. 3d and f).

The largest precipitation event in the studied period occurred in 30–31 Oct 2007 (26 mm in 27 h) producing the highest simulated discharge peak. During this period the simulated drains removed 4–16 mm of water while the measured cumulative drain discharge was 7 mm. The highest measured discharge peak in 2007 (0.32 mm h^{-1}) was clearly lower than the highest peaks in 2008 and 2012 (0.39–0.46 mm h^{-1}). This likely reflects the increasing drainage capacity of the field due to the supplementary drain installation. The maximum measured peak decreased from 0.46 mm h^{-1} in 2008 to 0.39 mm h^{-1} in 2012 but lower precipitation amounts during the 2012 period were responsible for the lower discharge peaks.

The hydrological effect of soil spatial heterogeneity was analyzed by parameterizing each cell with the properties of a randomly selected soil sample from the corresponding depth. Fig. 4 shows the average hourly drain discharge of five randomizations for both model configurations. The randomization was different for each model run, but the simulation results between the different model runs remained similar to each other. Also the hydrographs for different model configurations were more similar to each other (Fig. 4 a and b) compared to the homogenous soil properties (Fig. 3). For the dual-permeability model configuration the simulations with randomized soil properties produced higher N-S efficiency numbers compared to the cases with homogeneous soil properties (Table 2).

4.2. Cumulative drain discharge changes before and after the supplementary drain installation

Cumulative drain discharge results for the 2007, 2008 and 2012 periods are presented in Fig 5. The discharge results simulated with the five soil sets (Table 1) are combined into a range graph by selecting the minimum and maximum values from each hour. The range graph illustrates how much the discharge results varied between the five different soil parameterizations and the two model configurations during the autumn periods. The variation in the discharge results simulated with the single pore system model was higher and the median of the results was in the upper part of the range graph. The results computed with the dual-permeability model were more similar between the different soil sets and the median was closer to the lower boundary of the graph than the single pore system results (Figs. 5b, 5d and 5f). Even though the drain discharge peaks simulated with the dual-permeability model were higher (Fig. 3), the cumulative discharge results were lower and closer to the measurements than the single pore system results (Fig. 5).

According to the single pore system results, the soil sample set C1 with the lowest saturated hydraulic conductivities (Table 1) constantly produced the lowest cumulative drain discharge values (25, 46, and 41 mm) during the three simulated periods. Soils with similar low permeability values beneath the tilled topsoil layer could also be responsible for the restricted drainage capacity in the field. This indicates that decreasing drain spacing or increasing the amount of gravel in drain trenches may not increase field drainage capacity if the drain discharge is restricted by the surrounding soil properties. When the C1 parameterization was applied in the dual-permeability model, the cumulative discharge results were clearly closer to the measurements than the simulations with the single pore system model (lower boundary of the cumulative drain discharge cloud in Figs. 5b, 5d and 5f).

The normalized drain discharge (drain discharge divided by precipitation) increased after the supplementary drain installation (Table 3). The difference between 2007 period and the two later periods is visible with both model configurations, but there was again more variation in the single pore system model results between the soil sets. The normalized discharge increased from 0.32 to 0.54 for the C1 set (Table 1) using single pore system model and the smaller drain spacing, which could indicate that supplementary drains increased drainage capacity.

4.3. Water balance results from 2008 period

The simulation results from the autumn 2008 period were further analyzed to decipher the differences in the water balances between the grids 1–3 in Figs. 2a–c and the different model configurations (Fig. 6). The water balances are composed of topsoil layer runoff, drain discharge and groundwater outflow.

The variation in the simulated water balances with the different soil sample sets (C1–C5 in Table 1) was clearly lower with the dual-permeability approach than with the single pore approach (Fig. 6).

The effect of the trench was visible when applying the single pore system model as there was a clear difference in runoff components between the grids 2 and 3 (with or without the trench parameterization in Fig. 6c and Fig. 6e). The drain discharge was higher and topsoil layer runoff was lower in results computed with grid 2 (Fig. 6c) compared to the results with grid 3 (Fig. 6e). The reason for this is that water was not able to flow from the topsoil layer to the subsurface drains due to the very low hydraulic conductivity value in the subsoil layer (arithmetic mean between soil sets is 0.007 m h^{-1}) when the trench was not present in the single pore system simulation. When using the C4 parameterization and the single pore system model the simulated water balances generated with grids 2 and 3 were similar due to the higher saturated hydraulic conductivity (0.03 m h^{-1}) of the subsoil layer compared to other sample sets (average conductivity of C1–3 and C5 is 0.002 m h^{-1}).

According to the results computed with the dual-permeability model, the effect of the trench was subtle, because the macropore domain was able to activate rapid preferential flow to drains in all soils (Figs. 6d and 6f). We assumed that water could first infiltrate vertically via preferential flow pathways down to the shallow groundwater table and then continue laterally into the subsurface drain.

The drain discharges from the original and supplementary drains are presented separately in Fig. 6. The drainpipes were parametrized similarly and although the hydraulic properties of the trenches (original and supplementary) were different in the simulations, drain discharge was evenly generated through both drains with grids 2 and 3 (Fig. 2b and 2c). The total drain discharge was similar between grids 1 and 2 that represented the 16 and 8 m drain spacings, respectively. The soil sets C4 and C5 have the highest saturated hydraulic conductivity values in the subsoil layer (Table 1) providing well conducting flow pathways for water to reach the trench and the drain, meaning that the different grids had smaller effects on the water balance components compared to the soil sets C1–C3. Our hypothesis, in which water initially flows laterally in the topsoil layer towards the drain trench and then vertically down in the trench towards the drainpipe, can be correct for the soil sets C1, C2 and C3 as the low saturated hydraulic conductivity beneath the tilled topsoil layer or plow pan layer (Table 1) resulted in relatively high amount of tilled topsoil layer runoff when using the grid without trench. The feature was not visible in the dual-permeability model results due to the dominant effect of the macropore domain on soil water flow.

5. Discussion

5.1. Hourly and cumulative drain discharge

Drain discharge data and the results of the two model configurations (dual-permeability and single pore system) were analyzed with the five different soil parameterizations (Table 1) that showed large spatial variation within the studied area. The simulation results indicate that the limited number of soil samples was enough to represent the variation of soil hydraulic properties in the field section as the minimum and maximum simulated drain discharge hydrographs encompassed the measured discharge during the three autumn periods. The highest simulated peaks computed with the dual-permeability and the single pore system models overestimated the measured peaks. This is in contrast with earlier field scale FLUSH simulations in subsurface drained clay soils, where modelled hourly drain discharge peaks were lower compared to the measurements (Nousiainen et al., 2015; Warsta et al., 2013).

The cumulative drain discharge results simulated with the dual-permeability model were more in line with the measurements and included less variation compared to the discharge computed with the single pore system model. Previously, Gärdenäs et al. (2006) reported overestimated drain discharge peaks simulated with dual-porosity and dual-permeability models compared to data, while the single porosity model underestimated the data, but the authors did not present cumulative results from the simulations. Their simulations were conducted with a 2-D computational grid using data from a glacial till field in southern Sweden. Models embedding descriptions of preferential flow processes have been noted to have a tendency to overestimate hourly and daily drain discharge (Klaus and Zehe, 2010; Vogel et al., 2000). Haws et al. (2005) reported that the single pore system model produced higher discharge peaks than the dual-porosity model when simulating water flow in a 2-D grid with laterally homogeneous soil properties representing 3-D heterogeneous soil with macropore paths. Turunen et al. (2013) simulated the same Nummela field section as in this study with FLUSH assuming horizontally homogeneous soil layer properties. Even though they did not parameterize the drain trenches, the simulation results for drain discharge generated mainly by preferential flow were deemed to be successful.

The measured hourly drain discharges were characterized by blunt peaks during 2008 and 2012 periods (Fig. 3), which indicated that drain discharge rates in the field section were restricted to a maximum intensity (0.46 mm h^{-1} in 2008). The average soil moisture measured from nine locations was near saturation in the beginning of 2008 and 2012 simulation periods. Blunting of the peaks could have been caused by the wet field conditions prior to the simulation periods, but also by the low hydraulic conductivities in the subsoil layers, due to lack of preferential flow pathways, flat topography of the field or by limited drainpipe capacity. In fact, the maximum intensities were in the order of the design value of 0.36 mm h^{-1} (1 l s^{-1} ha^{-1}) for the drainage system. According to the data of Turunen et al. (2013), the hourly drain discharge peaks were smaller in the reference field section without the supplementary drainage in the Nummela field but exhibited similar round shapes as our data. Henine et al. (2010) noticed from field observations that flow rates through drain pipes were limited due to pipe pressurization during intense rainfall events in a tile drained catchment. Henine et al. (2014) were able to simulate the phenomenon with a 2-D model coupled to a 1-D pipe flow description. Simulation of water flow in drain pipes have been tested in a few 3-D studies with different methods, e.g. by describing the pipe network explicitly with 1-D elements (De Schepper et al., 2015) or by using a well conducting soil layer emulating the effect of a drainage system (De Schepper et al., 2015; Rozemeijer et al., 2010). In this study the drain nodes work as sinks and water is immediately removed from the system as it enters the drainpipe. Based on our results and the previous studies, inclusion of a pipe flow model would likely improve the drain discharge generation process description of FLUSH.

5.2. Water balance and effect of the drain trench

The application of the model in drain spacing scale enabled us to explicitly parameterize the drain trench and the surrounding soils into computational grids and to assess the effects of the supplemental drain installation on water balance components in soils with different hydraulic properties. The new drains clearly increased normalized drain discharges during the 2008 and 2012 periods compared to the period before the installation (2007) (Table 3). The share of drain discharge from precipitation was in 2008 1.4 and in 2012 1.3 times the share in 2007. Aura (1990) reported that their groundwater level observations in autumn showed that groundwater table was 30 to 50 cm lower with the supplementary drain in a clay field. Filipović et al. (2014) conducted 2-D and 3-D simulations with HYDRUS 2D/3D to test the effects of different drainage approaches in a heavy clay soil and stated that also mole drainage was an efficient practice to improve field drainage. In our study, the drain trenches had a clear effect on water balance components when the results were simulated with the single pore system model (Fig.6c and 6e). The trenches had a much smaller effect on water balance results when the dual-permeability model was applied (Fig. 6d and 6f). Our results indicate that the effect of drain trenches can be taken into account by (1) explicitly parameterizing the trench into a computational grid in single pore system model applications or (2) by using a dual-permeability model without trench parameterization. Previous field scale studies with the FLUSH model have applied the latter method (e.g. Turunen et al., 2015a; b; 2013; Warsta et al., 2013; Nousiainen et al., 2015). When single pore system model is applied and the drain trenches are not present in computational grids, water cannot reach the drains (Fig. 6e) due to the low permeability of clayey soils. The practical implication of the results is that the importance of trench decreases in soils with direct macropore connections sustaining efficient preferential flow between field surface and subsurface drains.

5.3. The effect of soil heterogeneity on water flow

Turunen et al. (2015b) restricted the lateral saturated hydraulic conductivity of the macropore system in soil layers closer to the surface but left the deeper layers isotropic in their 3-D field-scale simulations of the Nummela field. We did not apply anisotropic hydraulic conductivities in the computations and it is possible that in the dual-permeability simulations water movement should be restricted in the lateral directions. Otherwise water can flow laterally without restrictions in the subsoil layers to the subsurface drains. Petersen et al. (2007) stated that the variation of the anisotropy of soil saturated hydraulic conductivity in different soil layers should be accounted when modelling agricultural fields and it could explain the heterogeneous flow evident at the field scale. Vogel et al. (2000) conducted numerical experiments to assess differences in simulated water flow and solute transport results between single pore system and dual-permeability models in 2-D transects. According to the authors, soil heterogeneity could be described with dual-permeability model or with random hydraulic conductivity fields, although field evidence would be needed to verify such parameterisations (Vogel et al., 2000). Haws et al. (2005) concluded based on their single and dual porosity model results that failure in simulations can be attributed to problems with representing 3-D soil domain as 2-D domain with homogeneous soil properties in lateral directions and misrepresentation of macropore paths. In this study, the results of computational grids with randomized hydraulic properties (Table 1), showed that the different versions of the single pore system and dual-permeability model grids produced similar results and the results produced by the two model configurations were also similar. The N-S coefficient values were higher when grids with random hydraulic properties were applied in the simulations instead of homogeneous soil layers. This indicates that our method was able to describe some features of the heterogeneity present in the soil. Both single pore system and dual-permeability models produce comparable results against measurements, when the model is parameterized at a finer scale than drain spacing and the parameterization describes highly conductive subdomains of soil (i.e. macropore pathways or trenches). Taskinen et al. (2008) described a way to create random isotropic and anisotropic conductivity fields and the authors suggested that the solution should be easy to implement also in 3-D grids. Their approach could be used to further develop the simple randomization method applied in this study.

5.4. Model parameterization based on field data measurements and future objectives

The available soil data from Nummela were sparse but sufficient to demonstrate the impacts of different subsurface drainage methods and soil heterogeneity on discharge generation. The model performance was assessed with a single outflow variable following other model applications that use a similar approach in model calibration (e.g. De Schepper et al., 2015; Henine et al., 2010; Haws et al., 2005). Haws et al. (2005) stated that assessing model success by matching simulated and measured hydrographs for single outlet should be done with caution since observations from a single outlet may not contain enough information of the other hydrological processes within the field. Direct measurements of flow routes would be more useful than an aggregated discharge measurements for the calibration of spatially variable model parameters (Rozemeier et al., 2010). The groundwater table level observations provide another measure for monitoring the functioning of drainage systems even though modelling groundwater table level in clay soils is reported to be difficult (e.g. Aura, 1995). We were able to simulate the generation of drain discharge with a single pore system model although it has been noticed that single pore system models cannot accurately describe solute transport in clay soils (e.g. Gärdenäs et al., 2006; Haws et al., 2005). To track the water flow pathways with tracers, model configurations should be tested with solute transport simulations.

6. Conclusions

The drain discharge data and simulation results with the single pore system and dual-permeability models and different soil parameterizations were analyzed to decipher the impacts of different subsurface drainage methods, model structures and soil heterogeneity on drain discharge generation and water balance. Our results demonstrate that it was possible to produce plausible simulation results with both single pore system and dual-permeability models when the model was parameterized at a much finer scale than drain spacing and the parameterization described highly conductive subdomains such as macropores in the dual-permeability model or the trench in the single pore system model. If the trench is not described, a single point sample might not be enough to parameterize single pore system type models for clay since the water balance results simulated with the single pore system model were sensitive to soil hydraulic parameter values. Parameterization based on a single soil sample may lead to biased results, when the sample represents outermost range of soil conditions. Based on our simulation results with random sampling of soil data, heterogeneity of clay soil should be taken into account in model parameterization. Inclusion of more output variables in the simulations can further enhance the reliability of the model results, as the drain discharge data was not sufficient to determine the differences in the water flow pathways between the single pore system and dual-permeability models. The main novelty value of the results lies in the theoretical description and data-driven numerical experiments of field water balance facilitated by the 3-D FLUSH model. The water balance results have practical implication on implementation of drainage through the finding that gravel trench appears to be important only in soils with poorly conductive subsoil layers without direct macropore connections to subsurface drains.

Acknowledgments

The study was conducted in the TOSKA (*Functioning of drainage practices in crop production fields*) project (2014–2017) in which the functioning and the effects of different drainage methods on crop production, water balance and nutrient loads have been investigated. The study was funded by the Aalto University School of Engineering, Drainage Foundation sr, the Ministry of Agriculture and Forestry, Maa- ja vesitekniikan tuki ry., the Sven Hallin Research Foundation, Natural Resources Institute of Finland and Academy of Finland. We acknowledge CSC – IT Center for Science Ltd. for the allocation of computational resources.

References

Abrahamsen, P., Hansen, S., 2000. Daisy: an open soil-crop-atmosphere system model. Environ Modell. Softw., 15, 313-330.

Äijö H., Myllys, M., Nurminen, J., Turunen, M., Warsta, L., Paasonen-Kivekäs, M., Korpelainen, E., Salo, H., Sikkilä, M., Alakukku, L., Koivusalo, H., Puustinen, M., 2014. PVO2-hanke. Salaojitustekniikat ja pellon vesitalouden optimointi [Field drainage methods and optimizing water management of agricultural fields (PVO2)]. Salaojituksen tutkimusyhdistys ry:n tiedote 31. Finnish Field Drainage Association, Helsinki, Finland, 105 pp (in Finnish with English abstract).

Alakukku, L., Nuutinen, V., Ketoja, E., Koivusalo, H., Paasonen-Kivekäs, M., 2010. Soil macroporosity in relation to subsurface drain location on a sloping clay field in humid conditions. Soil Till. Res., 106, 275–284.

Alakukku, L., Weisskopf, P., Chamen, W.C.T., Tijink, F.G.J., van der Linden, J.P., Pires, S., Sommer, C., Spoor, G., 2003. Prevention strategies for field traffic-induced subsoil compaction: a review: Part 1. Machine/soil interactions. Soil Till. Res., 73, 145–160.

Allen, R., Pereira, L., Raes, D., Smith, M., 1998. Crop evapotranspiration – Guidelines for computing crop water requirements – FAO Irrigation and drainage paper 56. Rome: FAO – Food and Agriculture Organization of the United Nations. ISBN 92-5-104219-5. Available: http://www.fao.org/docrep/x0490e/x0490e00.htm.

An, H., Noh, S. J., 2014. High-order averaging method of hydraulic conductivity for accurate soil moisture modeling. J. Hydrol., 516, 119–130.

Aura, E., 1990. Salaojien toimivuus savimaassa. Tiedote 10/90. MTT Agrifood Research Finland, Jokioinen, Finland, 93 pp. ISSN: 0359–7652.

Aura, E., 1995. Finite element modeling of subsurface drainage in Finnish heavy clay soils. Agric. Water Manage., 28, 35–47.

Beven, K., Germann, P., 2013. Macropores and water flow in soils revisited. Water Resour. Res., 49, 3071–3092.

Blake, K.R., Hartge, K.H., 1986. Bulk density. In: Klute, A.K. (Eds.). Methods of soil analysis. Agronomy 9, Part 1: 363–375.

Brunner, P., Simmons, C. T., 2012. HydroGeoSphere: a fully integrated, physically based hydrological model. Ground Water, 50, 170–176.

Danielson, R.E., Sutherland, P.I., 1986. Porosity. In: Klute, A.K. (Eds.). Methods of soil analysis. Agronomy, Part 1: 443–461.

Danish Hydraulic Institute (DHI), 2007, The MIKE SHE User Manual, Volume 2: Reference Guide, Hørsholm, Denmark.

De Schepper, G., Therrien, R., Refsgaard, J. C., Hansen, A. L., 2015. Simulating coupled surface and subsurface water flow in a tile-drained agricultural catchment. J. Hydrol., 521, 374–388.

Feddes, R.A., Kowalik, P.J., Zaradny, H., 1978. Simulation of Field Water Use and Crop Yield. Pudoc, Wageningen, The Netherlands, 189 pp.

Filipović, V., Mallmann, F.J.K.,Coquet, Y., Šimůnek, J., 2014. Numerical simulation of water flow in tile and mole drainage systems. Agric. Water Manage.146: 105–114.

Frey, S. K., Hwang, H. T., Park, Y. J., Hussain, S. I., Gottschall, N., Edwards, M., Lapen, D. R., 2016. Dual permeability modeling of tile drain management influences on hydrologic and nutrient transport characteristics in macroporous soil. J. Hydrol., 535, 392–406.

Gärdenäs, A,, Šimůnek, J., van Genuchten, M.T., 2006. Two-dimensional modelling of preferential water flow and pesticide transport from a tile-drained field. J. Hydrol., 329, pp. 647–660.

Gerke H.H., Van Genuchten M.T., 1993. A dual-porosity model for simulating the preferential movement of water and solutes in structured porous media, Water Resour. Res. 29, pp. 305–319.

Hansen, A.L., Refsgaard, J.C., Christensen, B.S.B., Jensen, K.H., 2013. Importance of including small-scale tile drain discharge in the calibration of a coupled groundwater-surface water catchment model. Water Resour. Res. 49, 585–603.

Haws, N. W., Rao, P. S. C., Simunek, J., Poyer, I. C., 2005. Single-porosity and dual-porosity modeling of water flow and solute transport in subsurface-drained fields using effective field-scale parameters. J. Hydrol., 313, 257–273.

Henine, H., Nédélec, Y., Ribstein, P., 2014. Coupled modelling of the effect of overpressure on water discharge in a tile drainage system. J. Hydrol., 511, 39–48.

Henine, H., Nédélec, Y., Augeard, B., Birgand, F., Chaumont, C., Ribstein, P., Kao, C., 2010. Effect of pipe pressurization on the discharge of a tile drainage system. Vadose Zone J. 9, 36–42.

IUSS Working Group WRB, 2014. World Reference Base for Soil Resources 2014. International soil classification system for naming soils and creating legends for soil maps (PDF) (3rd ed.). Rome: FAO. ISBN 978-92-5-108370-3. Retrieved 29 August 2014.

Jansson, P. E., Karlberg, L., 2004. COUP manual: Coupled heat and mass transfer model for soil-plant-atmosphere systems. Technical manual for the CoupModel, 1–453.

Jarvis, N. J., 2007. A review of non-equilibrium water flow and solute transport in soil macropores: Principles, controlling factors and consequences for water quality. Eur. J. Soil Sci, 58, 523–546.

Jarvis, N., Larsbo, M., 2012. MACRO (v5. 2): Model use, calibration, and validation. Transactions of the ASABE, 55, 1413–1423.

Klaus, J., Zehe, E., 2010. Modelling rapid flow response of a tile-drained field site using a 2D physically based model: assessment of 'equifinal' model setups. Hydrol. Process., 24, 1595–1609.

Köhne, J. M., Mohanty, B. P., 2006. Water flow processes in a soil column with a cylindrical macropore: Experiment and hierarchical modeling. Water Resour. Res., 41.

Leij, F.J., Alves, W.J., van Genuchten, M.Th., Williams, J.R., 1996. Unsaturated Soil Hydraulic Database, UNSODA 1.0 User's Manual. Report EPA/600/R-96/095, US Environmental Protection Agency, Ada, Oklahoma, 103 pp.

Message P Forum, 1994. Mpi: a Message-Passing Interface Standard. Technical Report. University of Tennessee, Knoxville, TN, USA.

Messing, I., Wesström, I., 2006. Efficiency of old tile drain systems in soils with high clay content: Differences in the trench backfill zone versus the zone midway between trenches. Irrigation and drainage, 55, 523–531.

Nash, J.E., Sutcliffe, J.V., 1970. River flow forecasting through conceptual models part I — A discussion of principles. J. Hydrol., 10, 282–290.

Nielsen, M. H., Petersen, C. T., Hansen, S., 2015. Identification of efficient transport pathways from the soil surface to field drains by smoke injection. Eur. J. Soil Sci., 66, 516–524.

Nousiainen, R., Warsta, L., Turunen, M., Huitu, H. Koivusalo, H., Pesonen, L., 2015. Analyzing subsurface drain network performance in an agricultural monitoring site with a three-dimensional hydrological model. J. Hydrol., 529, 82–93.

Nuutinen, V., Butt, K. R., 2003. Interaction of Lumbricus terrestris L. burrows with field subdrains: The 7th international symposium on earthworm ecology· Cardiff· Wales· 2002. Pedobiologia, 47, 578–581.

Petersen, C. T., Trautner, A., Hansen, S., 2007. Spatio-temporal variation of anisotropy of saturated hydraulic conductivity in a tilled sandy loam soil. Soil Till. Res., 100, 108–113.

Ritzema, H. P., Nijland, H. J., Croon, F. W., 2006. Subsurface drainage practices: From manual installation to large-scale implementation. Agric. Water Manage., 86, 60–71.

Rozemeijer, J.C., van der Velde, Y., McLaren, R.G., van Geer, F.C., Broers, H.P., Bierkens, M.F.P., 2010. Integrated modeling of groundwater–surface water interactions in a tile-drained agricultural field: The importance of directly measured flow route contributions. Water Resour. Res., 46, W11537, DOI: 10.1029/2010WR009155.

Salo, H., Warsta, L., Turunen, M., Paasonen-Kivekäs, M., Nurminen, J., Koivusalo, H., 2015. Development and application of a solute transport model to describe field-scale nitrogen processes during autumn rains. Acta Agr Scand., Section B—Soil & Plant Science, 65(sup1), 30–43.

Shipitalo, M. J., Nuutinen, V., Butt, K. R., 2004. Interaction of earthworm burrows and cracks in a clayey, subsurface-drained, soil. Applied Soil Ecology, 26, 209–217.

Šimůnek, J., van Genuchten, M., 2008. Modeling nonequilibrium flow and transport processes using HYDRUS, Vadose Zone J., 7, 782–797.

Skaggs, R. W., 1980. DRAINMOD reference report. Washington, DC: USDA Soil Conservation Service.

Stuyt, L.C.P.M., Dierickx, W., Martínez Beltrán, J., 2005. Materials for subsurface drainage systems. FAO irrigation and drainage paper 60, rev. 1. FAO, Rome, Italy, 202 pp. Available at: ftp://ftp.fao.org/agl/aglw/docs/idp60.pdf

Taskinen, A., Sirviö, H., Bruen, M., 2008. Generation of two-dimensionally variable saturated hydraulic conductivity fields: model theory, verification and computer program. Comput. Geosci., 34, 876–890.

Turtola, E., Paajanen, A., 1995. Influence of improved subsurface drainage on phosphorus losses and nitrogen leaching from a heavy clay soil. Agric. Water Manag., 28, 295–310.

Turtola, E., Alakukku, L., Uusitalo, R., 2007. Surface runoff, subsurface drainflow and soil erosion as affected by tillage in a clayey Finnish soil, Agric. and Food Sci., 16, 332–351.

Turunen, M., Warsta, L., Paasonen-Kivekäs, M., Nurminen, J., Myllys, M., Alakukku, L., Äijö, H., Puustinen, M., Koivusalo, H., 2013. Modeling water balance and effects of different subsurface drainage methods on water outflow components in a clayey agricultural field in boreal conditions. Agric. Water Manage., 121, pp. 135–148.

Turunen, M., Warsta, L., Paasonen-Kivekäs, M., Nurminen, J., Alakukku, L., Myllys, M., Koivusalo, H., 2015a. Effects of terrain slope on long-term and seasonal water balances in clayey, subsurface drained agricultural fields in high latitude conditions. Agric. Water Manage., 150, 139–151.

Turunen, M., Warsta, L., Paasonen-Kivekäs, M., Nurminen, J., Koivusalo, H., 2015b. Simulating water balance and evapotranspiration in a subsurface drained clayey agricultural field in high-latitude conditions. Acta Agr Scand, Section B—Soil & Plant Science, 65(sup1), 44–57.

Vakkilainen, P., Alakukku, L., Myllys, M., Nurminen, J., Paasonen-Kivekäs, M., Peltomaa, R., Puustinen, M., Äijö, H., 2008. Pellon vesitalouden optimointi – Väliraportti 2008. Salaojituksen tutkimusyhdistys ry:n tiedote 29. Helsinki: Salaojituksen tutkimusyhdistys ry. 100 pp. ISBN 978-952-5345-21-6.

Vakkilainen, P., Alakukku, L., Koskiaho, J., Myllys, M., Nurminen, J., Paasonen-Kivekäs, M., Peltomaa, R., Puustinen, M., Äijö, H., 2010. Pellon vesitalouden optimointi - Loppuraportti 2010. Salaojituksen tutkimusyhdistys ry:n tiedote 30. Helsinki: Salaojituksen tutkimusyhdistys ry. 114 pp. ISBN 978-952-5345-23-0.

van Dam, J.C., Groenendijk, P., Hendriks, R.F.A., Kroes, J.G., 2008. Advances of modeling water flow in variably saturated soils with SWAP. Vadose Zone J., 7, 640–653.

van Genuchten, M.T., 1980. A closed form equation for predicting the hydraulic conductivity of unsaturated soils. Soil Sci. Soc. Am. J., 44, 892–898.

Vogel, T., Gerke, H., Zhang, R., van Genuchten, M., 2000. Modeling flow and transport in a two-dimensional dual-permeability system with spatially variable hydraulic properties, J. Hydrol., 238, 78–89.

Warsta, L., Turunen, M., Koivusalo, H., Paasonen-Kivekäs, M., Karvonen, T., Taskinen, A., 2012. Modelling heat transport and freezing and thawing processes in a clayey, subsurface drained agricultural field. 11th ICID Int. Drainage Workshop on Agricultural Drainage Needs and Future Priorities. Cairo 23-27.9.2012, Egypt. Proceedings. 10 pp.

Warsta, L., Karvonen, T., Koivusalo, H., Paasonen-Kivekäs, M., Taskinen, A., 2013. Simulation of water balance in a clayey, subsurface drained agricultural field with three-dimensional FLUSH model. J. Hydrol., 476, pp. 395–409.

Williams, J., Shaykewich, C.F., 1969. An evaluation of polyethylene (P.E.G.) 6000 and 20000 in the osmotic control of soil water matric potential. Can. J. Soil Sci., 49: 397–401.

Young, D. M., 2014. Iterative solution of large linear systems. Elsevier.

Youngs, E.G., 1991. Hydraulic conductivity of saturated soils. In: Smith, K.A.,Mullins, C.E. (Eds.). Soil analysis. Physical methods. 1991. 620 s.

Table 1. Soil hydraulic and structural properties for both model configurations (single pore system and dual-permeability models). θ_s and θ_r are the saturated and residual water contents, w is the macroporosity, K_{sat} is the saturated hydraulic conductivity, α and n are the van Genuchten water retention curve parameters and $K_{FS,MUL}$ is the macropore saturated hydraulic conductivity multiplier.

Table 2. Nash-Sutcliffe efficiency numbers for single pore system and dual-permeability model with homogeneous and randomized soil scenarios in 2008 autumn periods.

Table 3. Measured and simulated cumulative drain discharge results computed with the 16 m (2007) and 8 m (2008, 2012) drain spacings. The cumulative drain discharge [mm] is presented in parentheses and the percentage columns describe the drain discharge fraction of precipitation. Simulated values are presented as median [%] and minimum and maximum values [mm] computed with the five soil sets.

Figure 1. a) A map of Finland with the location of the Nummela field and b) detailed map of the C section in the field (original and supplementary drains, soil sample locations and the locations of groundwater observation wells, TDR sensors and measurement center).

Figure 2. Conceptual model setup of (a) a computational grid with original trench and surrounding soil (Grid 1), (b) a grid with original and supplementary drain trenches (Grid 2) and (c) a computational grid without trenches (Grid 3). The original tile drain trench is colored red (a and b) and the supplementary trench is colored gray (b). The grid dimensions are shown in the upper left corner of the figure.

Figure 3. Hourly measured and median of the simulated drain discharge results simulated with the single pore (a–c) and dual-permeability models (d–f) during 2007 (a and d), 2008 (b and e) and 2012 periods (c and f). The Nash-Sutcliffe model efficiency coefficients (NS) are presented for each event.

Figure 4. Hourly drain discharge with randomized soil hydraulic properties using a) single pore system model and b) dual-permeability model for autumn 2008 period. The blue line is the average of 5 randomization results and the black line is the measured hourly drain discharge.

Figure 5. Cumulative precipitation, measured cumulative drain discharge and simulated cumulative drain discharge computed with the single pore system (a, c and e) and dual-permeability (b, d and f) models during the 2007 (a and b), 2008 (c and d) and 2012 (e and f) periods. The simulated

cumulative discharge results computed with the five soil parameterizations are presented as range graphs.

Figure 6. Water balance components for the 2008 period computed with a) grid 1 and single pore system model, b) grid 1 and dual-permeability model, c) grid 2 and single pore system model, d) grid 2 and dual-permeability model, e) grid 3 and single pore system model and f) grid 3 and dual-permeability model.

Table 1. Soil hydraulic and structural properties for both model configurations (single pore system and dual-permeability models). θ_s and θ_r are the saturated and residual water contents, w is the macroporosity, K_{sat} is the saturated hydraulic conductivity, α and n are the van Genuchten water retention curve parameters and $K_{FS,MUL}$ is the macropore saturated hydraulic conductivity multiplier.

		Hydraulic parameters					Structure	
layer depth [m]	Soil set	α [1/m]	n [-]	K_{sat} [m/h]	θ_R [m³/ m³]	θ_S [m³/ m³]	w [-]	$K_{FS,MUL}$ [m/h]
0–0.25	C1	0.65	1.16	0.032	0.1	0.52	0.011	80
	C2	2.3	1.17	0.18	0.1	0.48	0.13	10
	C3	13.0	1.12	0.57	0.1	0.53	0.074	10
	C4	2.9	1.15	0.059	0.1	0.55	0.055	19
	C5	4.0	1.15	0.18	0.1	0.56	0.067	39
0.25–0.45	C1	0.12	1.30	0.0012	0.1	0.59	0.002	80
	C2	0.96	1.10	0.26	0.1	0.52	0.0057	80
	C3	0.54	1.13	0.19	0.1	0.51	0.003	80
	C4	0.45	1.16	0.004	0.1	0.54	0.0064	80
	C5	0.46	1.17	0.00004	0.1	0.53	0.002	9
0.45–1.0	C1	0.44	1.13	0.00005	0.1	0.55	0.0025	5
	C2	0.62	1.14	0.00005	0.1	0.55	0.0011	40
	C3	0.96	1.13	0.0004	0.1	0.54	0.0027	55
	C4	0.74	1.13	0.03	0.1	0.53	0.0084	80
	C5	0.66	1.12	0.0063	0.1	0.50	0.0079	80
1.0–1.5	Bottom soil	0.68	1.16	0.00008	0.1	0.53	0.0006	80
0.25–1.0	Gravel [(a]	2.9	1.71	0.07	0.058	0.30	0.5	-
0–1.5	Macropores [(b]	20	2	-	0.01	-	-	-

[a)] Leij et al. (1996)

[b)] Köhne and Mohanty (2006)

Table 2. Nash-Sutcliffe efficiency numbers for single pore system and dual-permeability model with homogeneous and randomized soil scenarios in 2008 autumn periods.

	Single pore system model		Dual-permeability model	
	Homogenous	Randomized	Homogenous	Randomized
16.–21.10.2008	0.44	0.00	0.55	0.53
21.–26.10.2008	0.72	0.75	-0.06	0.67
26.–30.10.2008	0.27	0.20	-0.33	0.28
30.10.–7.11.2008	0.76	0.75	0.46	0.78

Table 3. Measured and simulated cumulative drain discharge results computed with the 16 m (2007) and 8 m (2008, 2012) drain spacings. The cumulative drain discharge [mm] is presented in parenthesis and the percentage columns describe the drain discharge fraction of precipitation. Simulated values are presented as median [%] and minimum and maximum values [mm] computed with the five soil sets.

	Measured		Single pore system model		Dual-permeability model	
	[%]	[mm]	Median [%]	(min–max) [mm]	Median [%]	(min–max) [mm]
2007	40	(26)	69	(22–56)	54	(35–47)
2008	60	(57)	94	(46–82)	78	(60–67)
2012	71	(44)	89	(41–57)	70	(39–45)

Figure

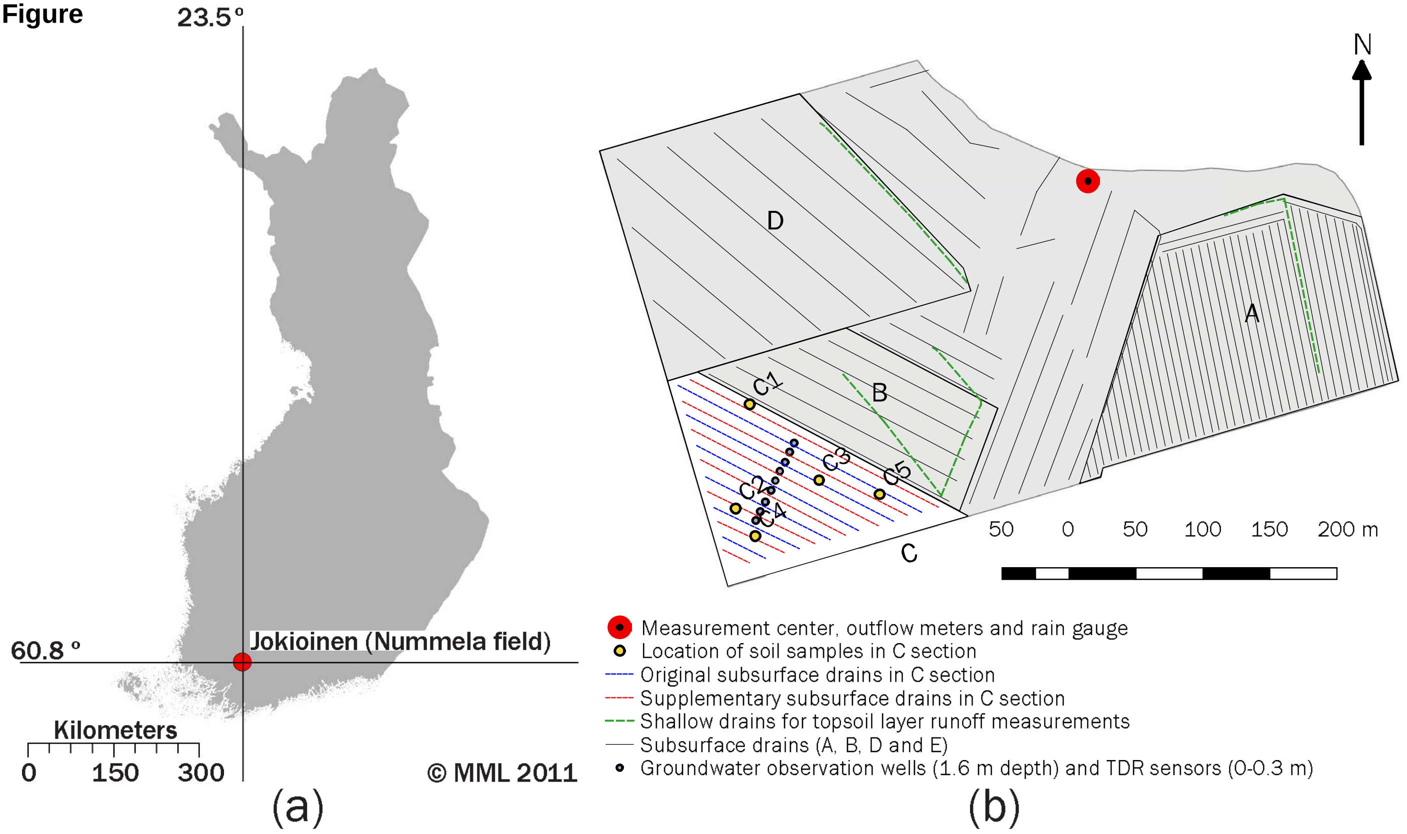

23.5 °
60.8 °
Jokioinen (Nummela field)
Kilometers
0
150
300
© MML 2011
(a)
N
D
A
B
C
C1
C2
C3
C4
C5
50
0
50
100
150
200 m
Measurement center, outflow meters and rain gauge
Location of soil samples in C section
Original subsurface drains in C section
Supplementary subsurface drains in C section
Shallow drains for topsoil layer runoff measurements
Subsurface drains (A, B, D and E)
Groundwater observation wells (1.6 m depth) and TDR sensors (0-0.3 m)
(b)

Figure

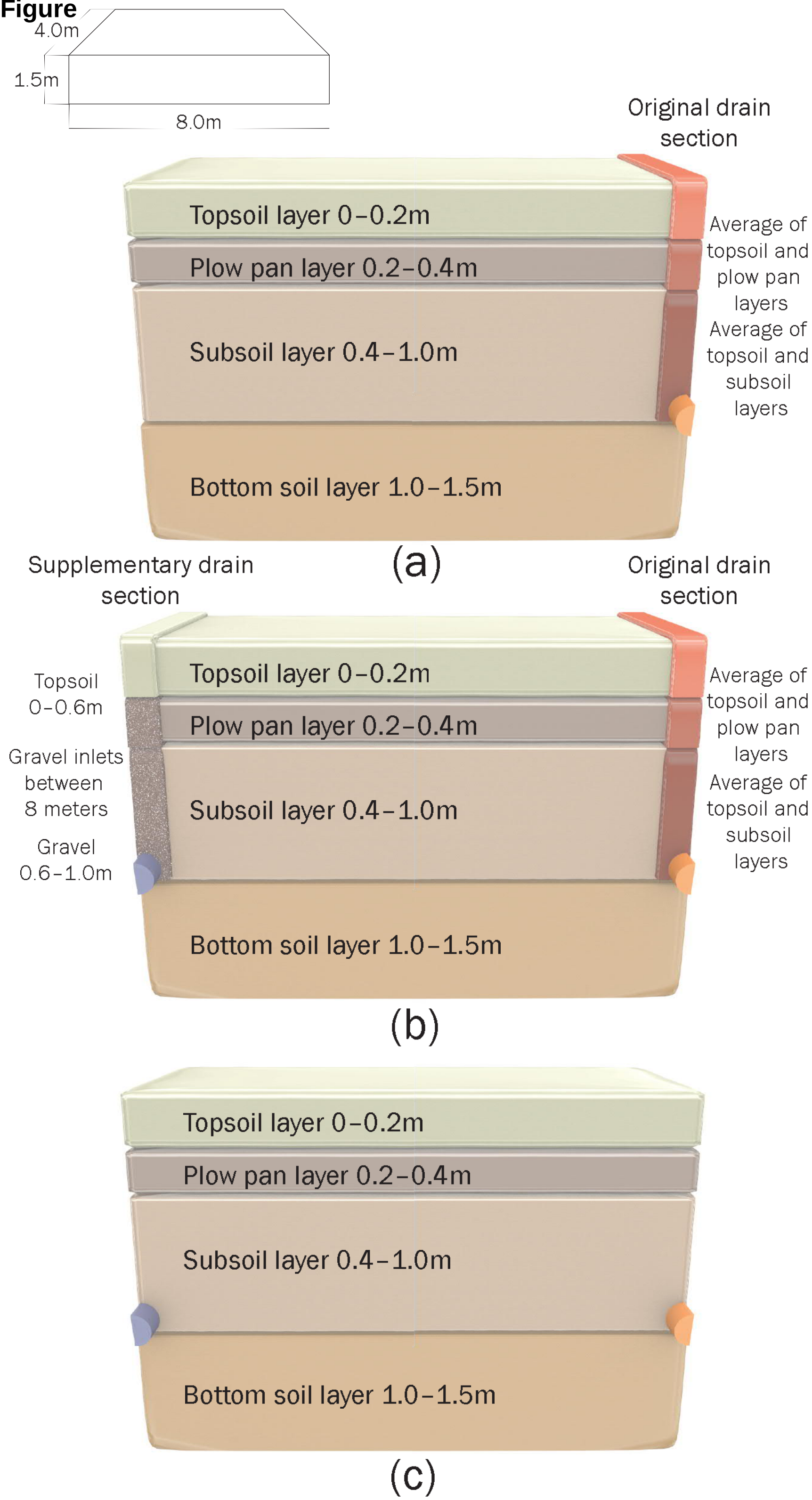

4.0m
1.5m
8.0m
Original drain section
Topsoil layer 0–0.2m
Plow pan layer 0.2–0.4m
Subsoil layer 0.4–1.0m
Bottom soil layer 1.0–1.5m
Average of topsoil and plow pan layers
Average of topsoil and subsoil layers
(a)
Supplementary drain section
Original drain section
Topsoil 0–0.6m
Gravel inlets between 8 meters
Gravel 0.6–1.0m
Topsoil layer 0–0.2m
Plow pan layer 0.2–0.4m
Subsoil layer 0.4–1.0m
Bottom soil layer 1.0–1.5m
Average of topsoil and plow pan layers
Average of topsoil and subsoil layers
(b)
Topsoil layer 0–0.2m
Plow pan layer 0.2–0.4m
Subsoil layer 0.4–1.0m
Bottom soil layer 1.0–1.5m
(c)

Figure

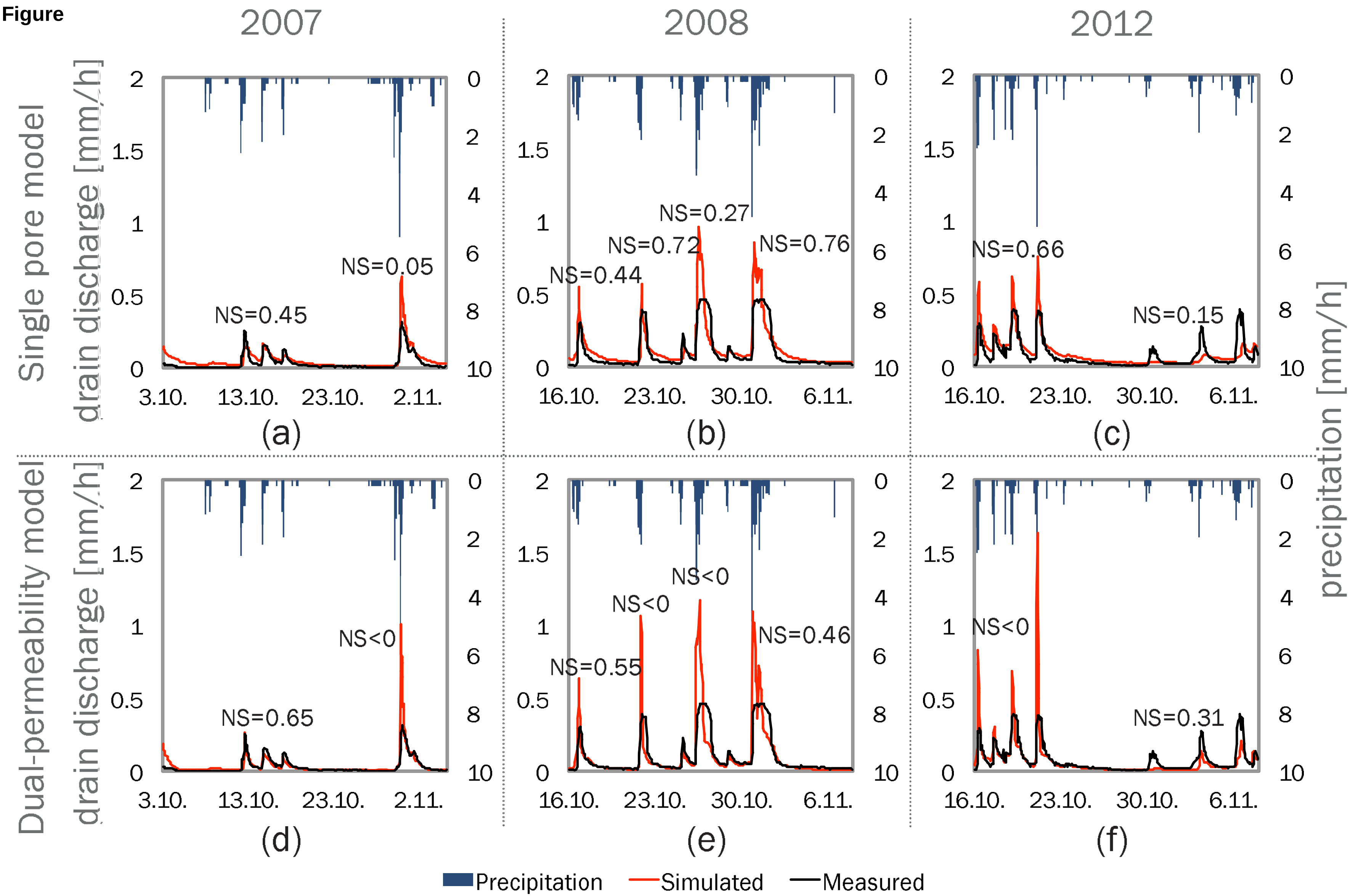

2007
2008
2012
Single pore model
Dual-permeability model
drain discharge [mm/h]
precipitation [mm/h]
NS=0.45
NS=0.05
NS=0.44
NS=0.72
NS=0.27
NS=0.76
NS=0.66
NS=0.15
NS=0.65
NS<0
NS=0.55
NS<0
NS<0
NS=0.46
NS<0
NS=0.31
3.10.
13.10.
23.10.
2.11.
16.10.
23.10.
30.10.
6.11.
(a)
(b)
(c)
(d)
(e)
(f)
Precipitation
Simulated
Measured

Figure

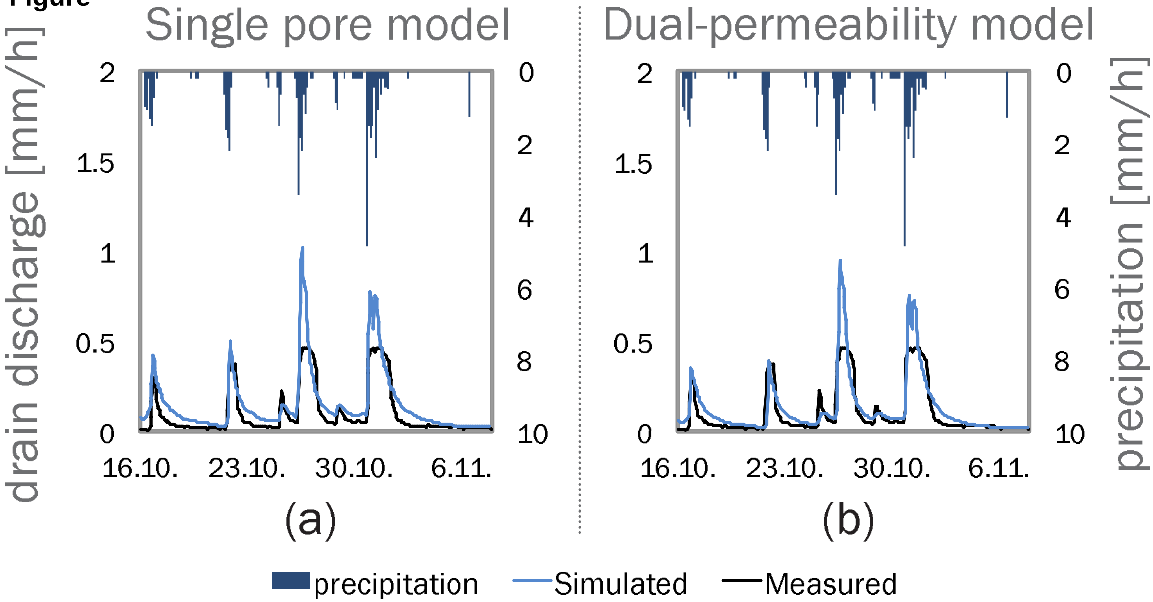

Single pore model
Dual-permeability model
drain discharge [mm/h]
precipitation [mm/h]
2
1.5
1
0.5
0
0
2
4
6
8
10
16.10.
23.10.
30.10.
6.11.
(a)
(b)
precipitation
Simulated
Measured

Figure

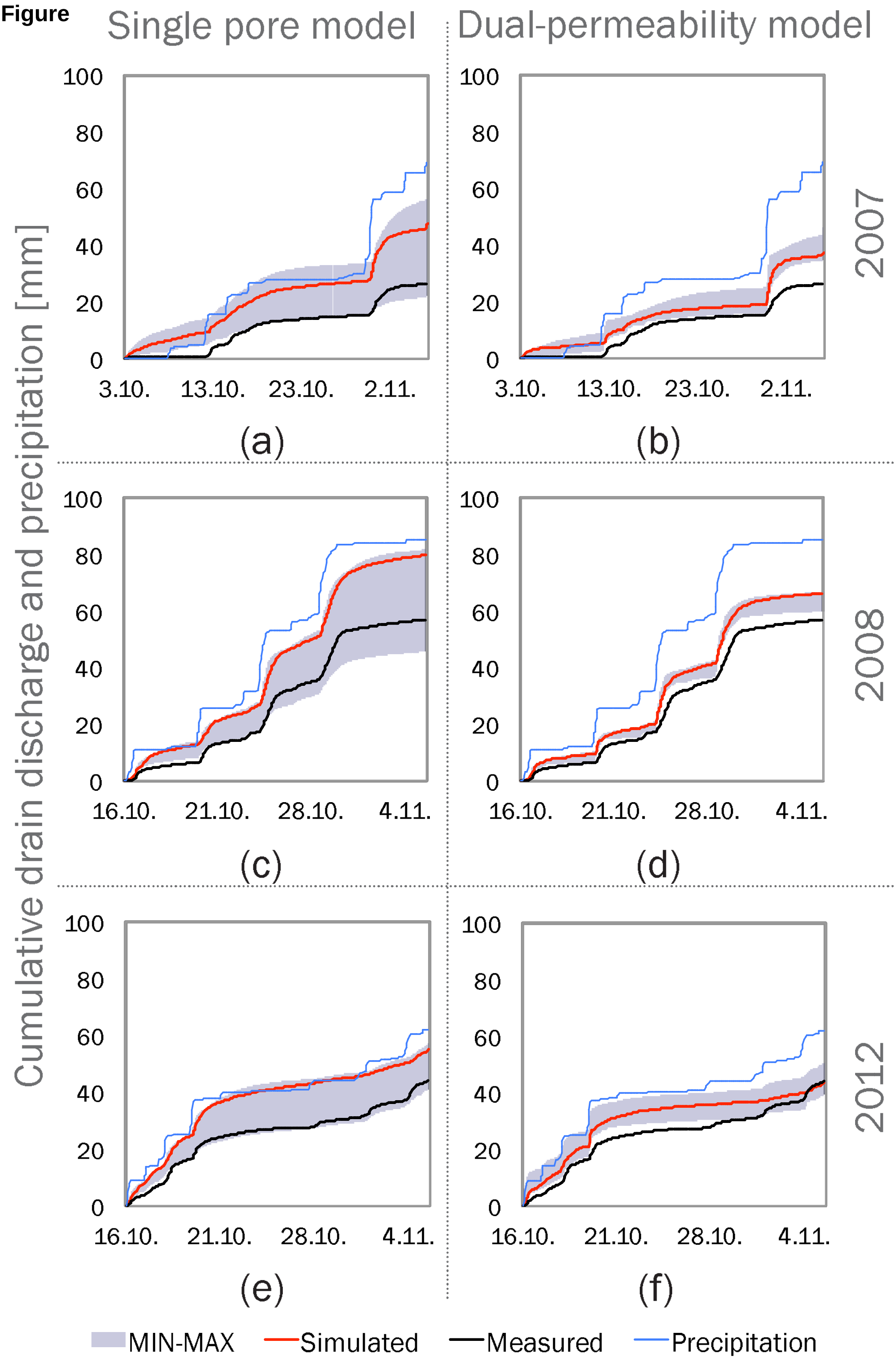

Single pore model
Dual-permeability model
Cumulative drain discharge and precipitation [mm]
2007
2008
2012
100
80
60
40
20
0
3.10.
13.10.
23.10.
2.11.
16.10.
21.10.
28.10.
4.11.
(a)
(b)
(c)
(d)
(e)
(f)
MIN-MAX
Simulated
Measured
Precipitation

Figure

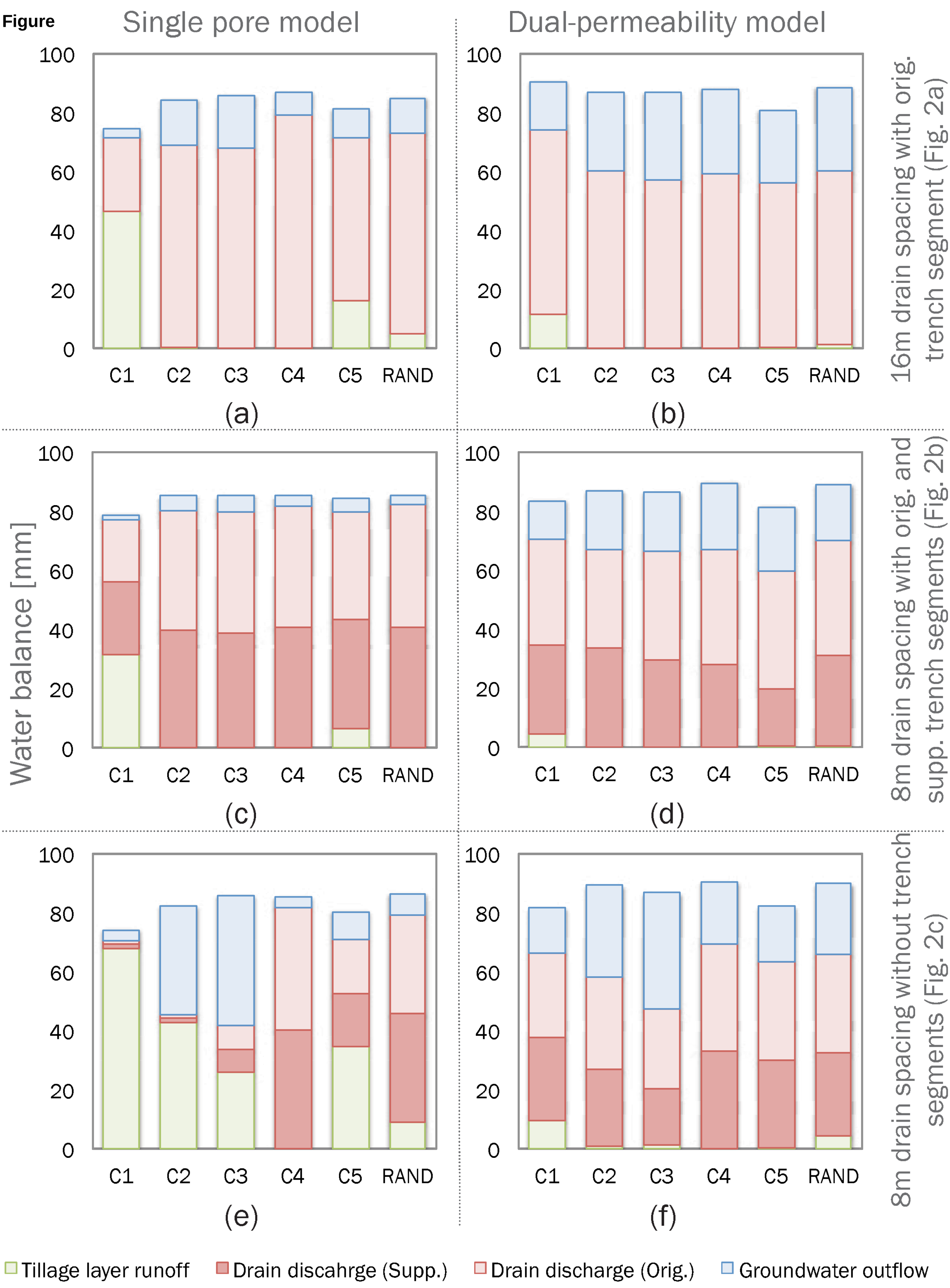
Single pore model
Dual-permeability model
Water balance [mm]
C1
C2
C3
C4
C5
RAND
(a)
(b)
(c)
(d)
(e)
(f)
16m drain spacing with orig. trench segment (Fig. 2a)
8m drain spacing with orig. and supp. trench segments (Fig. 2b)
8m drain spacing without trench segments (Fig. 2c)
Tillage layer runoff
Drain discahrge (Supp.)
Drain discharge (Orig.)
Groundwater outflow